

X-ray spectral properties of high-redshift radio-loud quasars beyond redshift 4—first results [★]

W. Yuan^{1†}, A.C. Fabian², M.A. Worsley², and R.G. McMahon²

¹*National Astronomical Observatories of China/Yunnan Observatory, Phoenix Hill, P.O. Box 110, Kunming, Yunnan, China*

²*University of Cambridge, Institute of Astronomy, Madingley Road, Cambridge, CB3 0HA*

Accepted Feb 9, 2006, Received ???

ABSTRACT

We present the results of X-ray spectroscopic observations with *XMM-Newton* for four high-redshift radio-loud quasars at $z > 4$. Among these, three objects, namely, GB B1508+5714, PMN J0324-2918, and PKS B1251-407 do not show soft X-ray spectral flattening; the derived upper limits on assumed intrinsic absorption are $(3.3 - 17.3) \times 10^{21} \text{ cm}^{-2}$, the least of which is among the most stringent limits for $z > 4$ quasars. There is a tentative indication for soft X-ray spectral flattening in PMN J1451-1512 at $z=4.76$, though the significance is not high. These observations more than double the number of $z > 4$ radio-loud quasars having X-ray spectroscopic data to seven, which compose a significant subset of a flux-limited sample of $z > 4$ radio-loud quasars. Based on this subset we show, in the second part of the paper, some preliminary results on the overall X-ray spectral properties of the sample. Soft X-ray spectral flattening, which is thought to arise from intrinsic X-ray absorption, was found in about half of the sample (3/7 or 4/7). We give a preliminary distribution of the absorption column density N_{H} . For those with detected X-ray absorption, the derived N_{H} values fall into a very narrow range (around a few times 10^{22} cm^{-2} for ‘cold’ absorption), suggesting a possible common origin of the absorber. This N_{H} distribution is consistent with that in the redshift range of 2–4, though the data are sparse. Those that do not show X-ray absorption are constrained to have upper limits on the N_{H} broadly consistent in general with the lower end of the distribution of the detected N_{H} . Compared to lower-redshift samples at $z < 2$, there is an extension, or a systematic shift, toward higher values in the intrinsic N_{H} distribution at $z > 4$, and an increase of the fraction of radio-loud quasars showing X-ray absorption toward high redshifts. These results indicate a cosmic evolution effect, which seems to be the strongest at redshifts around 2. There is a tentative tendency that objects showing X-ray absorption have X-ray fluxes systematically higher than those showing apparently no absorption. After the spectral flattening is accounted for, the rest frame 1–50 keV continua have photon indices with a mean of 1.64 and a standard deviation of 0.11 (or a mean of 1.67 and a standard deviation of 0.14 for a Gaussian fit). Variability appears to be common on timescales from a few months to years in the quasar rest-frame, sometimes in both fluxes and spectral slopes.

Key words: galaxies: active – galaxies: individual: GB B1508+5714 PMN J1451-1512 PMN J0324-2918 PKS B1251-407 – X-ray: galaxies

1 INTRODUCTION

Quasars with powerful radio emission are very rare in the early universe. Beyond redshift 4, only about a dozen quasars with 5 GHz fluxes brighter than 50 mJy are known so far (e.g. Hook & McMahon 1998, Hook et al. 2002, Snellen et al. 2002). X-ray spectroscopic observations on a few ob-

jects revealed some interesting features. Among these is the flattening of soft X-ray spectra towards low energies as observed in three objects GB B1428+4217, PMN J0525-3343, RX J1028.6-0844 (e.g. Boller et al. 2000, Yuan et al. 2000, 2005, Fabian et al. 2001ab, Worsley et al. 2004ab). Tentative evidence for the spectral flattening was also found in the combined spectra of several $z > 4$, moderately radio-loud quasars with *Chandra* (Bassett et al. 2004), but not in their radio-quiet counterparts (e.g. Vignali et al. 2003, 2005;

† E-mail: wmy@ynao.ac.cn

Grupe et al. 2006). In the lower redshift range $2 < z < 4$, this effect was also seen with *XMM-Newton* observations in several highly radio-loud quasars in, e.g. PKS 2126-0158 at $z=3.27$ (Ferrero & Brinkmann 2003) and RBS 315 at $z=2.69$ (Piconcelli & Guainazzi 2005), and some others as reported recently by Page et al. (2005) using archival data of *XMM-Newton*. In fact, similar results, though subject to relatively large uncertainties, had already been obtained with other X-ray astronomical satellites prior to *XMM-Newton* (e.g. Wilkes et al. 1992; Elvis et al. 1994, 1998; Cappi et al. 1997; Brinkmann et al. 1997; Fiore et al. 1998, 2003; Yuan & Brinkmann 1999; Reeves & Turner 2000). This effect is preferably explained as photoelectric absorption of soft X-rays (excess absorption), though an intrinsic spectral break cannot be ruled out. When fitted with ‘cold’ absorption models at the quasar redshifts, the column densities are around a few times 10^{22} cm^{-2} as measured in recent *XMM-Newton* observations¹. The nature of the absorbers (if indeed due to absorption) is not understood yet. In fact, it is not even known whether this effect is ubiquitous in objects of this kind. Another feature is that a few objects resemble blazars in many ways (e.g. Fabian et al. 1997, 1998), characterized by (apparently) very high X-ray luminosities and short timescale variability, in which the relativistic beaming effect plays a role. However, these results may not be representative of the population as only a few objects were sampled; more X-ray spectroscopic data are needed.

Furthermore, a sizable sample at $z > 4$ with good X-ray spectroscopic data will provide a basis for the studying of evolution of radio-loud quasars over a large span of cosmic look-back time. This is particularly relevant in the light of recent realization that at redshifts as high as 4 the cosmic microwave background radiation may start to dominate the seed photon field for inverse Compton processes responsible for the X-ray emission (Schwartz 2002). Such an example may have been seen as an X-ray jet/blob associated with one of these objects GB B1508+5714 at $z=4.3$ as discovered recently with Chandra (Yuan et al. 2003, Siemiginowska et al. 2003).

We compiled a flux-limited ($f_{5\text{GHz}} > 50 \text{ mJy}$) sample of radio-loud quasars at $z > 4$, which comprises of about a dozen objects, from recent high- z radio quasar surveys (e.g. Hook & McMahon 1998, Hook et al. 2002, Snellen et al. 2002). In this paper we, firstly, report on *XMM-Newton* observations of several more objects selected from the sample; secondly, discuss briefly the X-ray spectral properties of the sample by combining the new data with those published previously. It should be noted that these objects (listed in Table 1) represent a significant subset of the whole sample. The majority of the sample are highly radio-loud quasars (radio-loudness² $\gg 10^2$), as compared to those moderately radio-loud quasars at similar redshifts studied by Bassett et al. (2004) with Chandra, in which rather tentative evidence for intrinsic X-ray absorption was claimed. We adopt $H_0=71 \text{ km s}^{-1} \text{ Mpc}^{-1}$, $\Omega_A=0.73$, and $\Omega_m=0.27$. Errors and

upper limits are quoted at the 68 per cent level unless stated otherwise.

2 RESULTS OF NEW X-RAY OBSERVATIONS

2.1 Observations and data reduction

The observation logs are summarised in Table 2. Most of the new observations were taken in the *XMM-Newton* AO3 period, while GB B1508+5714 was observed previously in 2002. PMN J1451-1512 was observed twice at 5 month apart. All the EPIC (European Photon Imaging Camera) cameras MOS1, MOS2, and PN were active in the observations. The *XMM-Newton* Science Analysis System (SAS, v.6.1) and the most up-to-date calibration data³ (as of July 2005) were used for data reduction. We followed the standard data reduction and screening procedures. Exposure periods which suffered from high flaring background caused by soft protons were removed. The observation for PKS B1251-407 was affected most, and much higher cut-off thresholds for background flares than the recommended values (see Loiseau 2004)⁴ were adopted to ensure enough source counts for spectral analysis.

For all the objects the X-rays were detected at the quasar positions. Source counts were extracted from a circle of $32''$ radius (corresponding to the $\simeq 87$ per cent encircled energy radius). Background events were extracted from source-free regions using a concentric annulus for the MOS detectors, and one or more circles of $32''$ radius at the same CCD read-out column as the source position for the PN detector. X-ray images, light-curves, and spectra were generated from the extracted, cleaned events for the source and background. The data screening criteria and the source count rates are given in Table 2. The spectra were created using X-ray events of pattern 0–4 for PN and 0–12 for MOS, respectively, in the 0.2–8 keV band, and were re-binned to have a minimum of 25–30 counts in each bin. The EPIC response matrices (*rmf* and *arf*) were generated using the source information on the detectors.

2.2 X-ray spectra

We used XSPEC (v.11.3.1) for spectral fitting. For a given observation, the spectra obtained with the two MOS detectors were found to be highly consistent with each other, as expected, and thus were combined to form one single MOS spectrum. Furthermore, the PN and MOS detectors also yielded statistically consistent spectra. Therefore, for a given observation, joint spectral fitting was performed to the PN and the combined MOS spectra. The results of the spectral fits are summarised in Table 3. For PMN J1451-1512 the spectral fits were performed both to each observation individually and to the two observations jointly (1+2 in Table 3).

¹ Earlier observations with *ASCA* and *BeppoSAX* gave somewhat higher column densities; in this paper we take the *XMM-Newton* results whenever available, though the disagreement is not fully understood yet.

² Defined as the K -corrected ratio of radio (5 GHz) to optical (B -band) fluxes.

³ After we finished the work the new version of SAS (v.6.5) was released. We examined any possible effects of the new SAS version on our results but found no systematic inconsistency; the changes in the fitted spectral parameters are negligible compared to the statistical uncertainties of the measurement.

⁴ 1 cts s⁻¹ and 0.35 cts s⁻¹ for PN and MOS detectors, respectively; see Loiseau 2004.

Table 1. The sample of $z > 4$ radio-loud quasar observed with *XMM-Newton*

object	RA J2000	Dec	redshift	S _{5GHz} mJy	magnitude mag	references
PMN J1451–1512	14 51 47.05	–15 12 20.0	4.76	90	19.1(<i>R</i>)	Hook et al. 2002
PMN J0324–2918	03 24 44.28	–29 18 21.1	4.63	354	18.60(<i>R</i>)	Hook et al. 2002
PKS B1251–407	12 53 59.53	–40 59 30.7	4.46	220	19.9 (<i>i</i>)	Shaver et al. 1996
GB B1508+5714	15 10 02.92	+57 02 43.4	4.30	282	19.89(<i>i</i>)	Hook et al. 1995
Objects with <i>XMM-Newton</i> spectroscopic data published previously						
GB B1428+4217	14 30 23.74	+42 04 36.5	4.72	337	20.9	Worsley et al. 2004b
PMN J0525–3343	05 25 06.17	–33 43 05.5	4.41	210	18.7	Worsley et al. 2004a
RX J1028.6–0844	10 28 38.70	–08 44 38.8	4.27	159	21.0	Yuan et al. 2005

^a For PMN J1451–1512 and PMN J0324–2918 the positions refer to their APM *R* band optical positions (Hook et al. 2002). For PKS B1251–407 the radio VLBI position (Ma et al. 1998) is quoted.

Table 2. *XMM-Newton* observation logs, data screening criteria, and source detection

object (observation)	obs. id	date of obs.	filter	duration ks MOS/PN	bgd cutoff cts s ^{–1} MOS/PN	good exposure ks MOS/PN	count rate 10 ^{–2} cts s ^{–1} (0.2–8keV) MOS/PN
PMN J1451–1512	0204190101	2004-02-15	Medium	17.7/14.3	0.35/1.2	6.8/5.2	1.5±0.2/6.6±0.4
PMN J1451–1512	0204190401	2004-07-22	Medium	21.1/19.5	0.5/1.5	19.7/12.0	1.7±0.1/6.1±0.3
PMN J0324–2918	0204190201	2004-02-09	thin	13.1/11.5	0.35/1.0	5.8/4.6	1.1±0.2/4.4±0.3
PKS B1251–407	0204190301	2004-07-12	thin	21.8/19.6	3.0/15.0	17.6/10.5	1.3±0.2/3.6±0.5
GB B1508+5714	0111260201	2002-05-11	thin	13.2/10.9	0.3/1.0	12.0/9.3	4.2±0.2/15.6±0.4

^a For the MOS detectors the vaules quoted are of MOS1 (MOS2 has almost identical values with MOS1).

^b *bgd cutoff* means the cutoff threshold for flaring background caused by soft protons (for events with energy >10 keV).

All the spectra can be well described with models of power-law modified by ‘cold’ absorption. Statistically consistent results were obtained for the fits with the absorption column density N_{H} as either a free parameter or fixed at the Galactic value (Table 3). The X-ray spectra and the best-fit models with N_{H} fixed at the Galactic value are shown in Fig. 1. Plotted in Fig. 2 are the confidence contours, as derived for two interesting parameters, for the fitted absorption N_{H} in conjunction with the power law photon indices Γ . For PKS B1251–407 and PMN J0324–2918, the low spectral quality render relatively large uncertainties for the fitted parameters. The X-ray fluxes were calculated by assuming the best-fit power-law model with Galactic absorption for both the cases with and without the correction of Galactic absorption. The fluxes and the quasar rest frame luminosities are given in Table 4.

The immediate inference from these results is that, in general, there is no significant amount of excess absorption above the Galactic column density, though a moderate amount of such absorption cannot be ruled out for PMN J1451–1512. We thus added a redshifted absorption component at the quasar redshift in the above model and fixed the local absorption at the Galactic $N_{\text{H}}^{\text{Gal}}$. This yielded slight improvement in the fit with $\Delta\chi^2=3$ (for one additional parameter), and a best-fit excess absorption $N_{\text{H}} = (10.4^{+6.1}_{-5.8}) \times 10^{21} \text{ cm}^{-2}$. Fig. 3 shows the confidence contours for the intrinsic column density and the power-law photon

Table 4. X-ray fluxes and rest frame luminosities

object (observation)	flux ^{a)} 0.2–10 keV 10 ^{–13} erg s ^{–1} cm ^{–2}	flux ^{b)}	Luminosity 1–50 keV 10 ⁴⁶ erg s ^{–1}
PMN J1451–1512 (1)	2.00	2.50	5.82
PMN J1451–1512 (2)	2.12	2.61	6.07
PMN J0324–2918	1.32	1.39	2.98
PKS B1251–407	1.66	1.97	3.93
GB B1508+5714	5.29	5.55	10.2

^a Fluxes measured by using the fitted power-law model in the presence of Galactic absorption.

^b Same power-law model with a) but with Galactic absorption corrected. The values quoted are the mean of the MOS and PN results.

index for PMN J1451–1512. It is clear that the statistical significance is not high and thus the excess absorption is only indicative. It should be noted that almost identical results were obtained when fitting the data set of each individual observation of PMN J1451–1512. Assuming the absorber is ionised did not give a better fit over the ‘cold’ absorption model. For the three remaining objects, no excess N_{H} is required, leading to only upper limits (see Table 3).

Table 3. Results of X-ray spectral fits

object (observation)	$N_{\text{H}}^{\text{Gal}}$ 10^{21} cm^{-2}	Γ	χ^2/dof	N_{H} 10^{21} cm^{-2}	Γ	χ^2/dof	$N_{\text{H}}^{\text{exc}}$ 10^{21} cm^{-2}	Γ	χ^2/dof
PMN J1451–1512 (1)	0.78	1.78 ± 0.07	20/23	$0.98^{+0.24}_{-0.26}$	1.87 ± 0.10	20/22	$11.7^{+11.9}_{-11.2}$	1.87 ± 0.10	19/22
PMN J1451–1512 (2)	0.78	1.75 ± 0.05	58/57	0.93 ± 0.16	1.82 ± 0.07	57/56	$10.0^{+7.2}_{-7.1}$	1.83 ± 0.06	56/56
PMN J1451–1512 (1+2)	0.78	1.76 ± 0.04	78/81	0.94 ± 0.13	1.83 ± 0.05	77/80	$10.4^{+6.1}_{-5.8}$	1.84 ± 0.05	75/80
PMN J0324–2918	0.11	1.64 ± 0.09	17/17	$0.08^{+0.19}_{-0.08}$	$1.61^{+0.15}_{-0.11}$	17/16	< 6.5	$1.64^{+0.11}_{-0.09}$	17/16
PKS B1251–407	0.80	1.64 ± 0.11	32/29	0.97 ± 0.38	1.71 ± 0.15	32/28	< 17.2	1.66 ± 0.13	32/28
GB B1508+5714	0.16	1.51 ± 0.03	92/82	0.16 ± 0.06	1.51 ± 0.04	92/82	< 3.3	1.52 ± 0.04	92/81

a The spectral fits were performed jointly to the PN spectrum and the combined MOS1 and MOS2 spectra.

b $N_{\text{H}}^{\text{Gal}}$ is the Galactic column density toward the direction of a source; N_{H} is the fitted total local absorption column density; $N_{\text{H}}^{\text{exc}}$ refers to the column density of excess absorption; Γ is the power-law photon index.

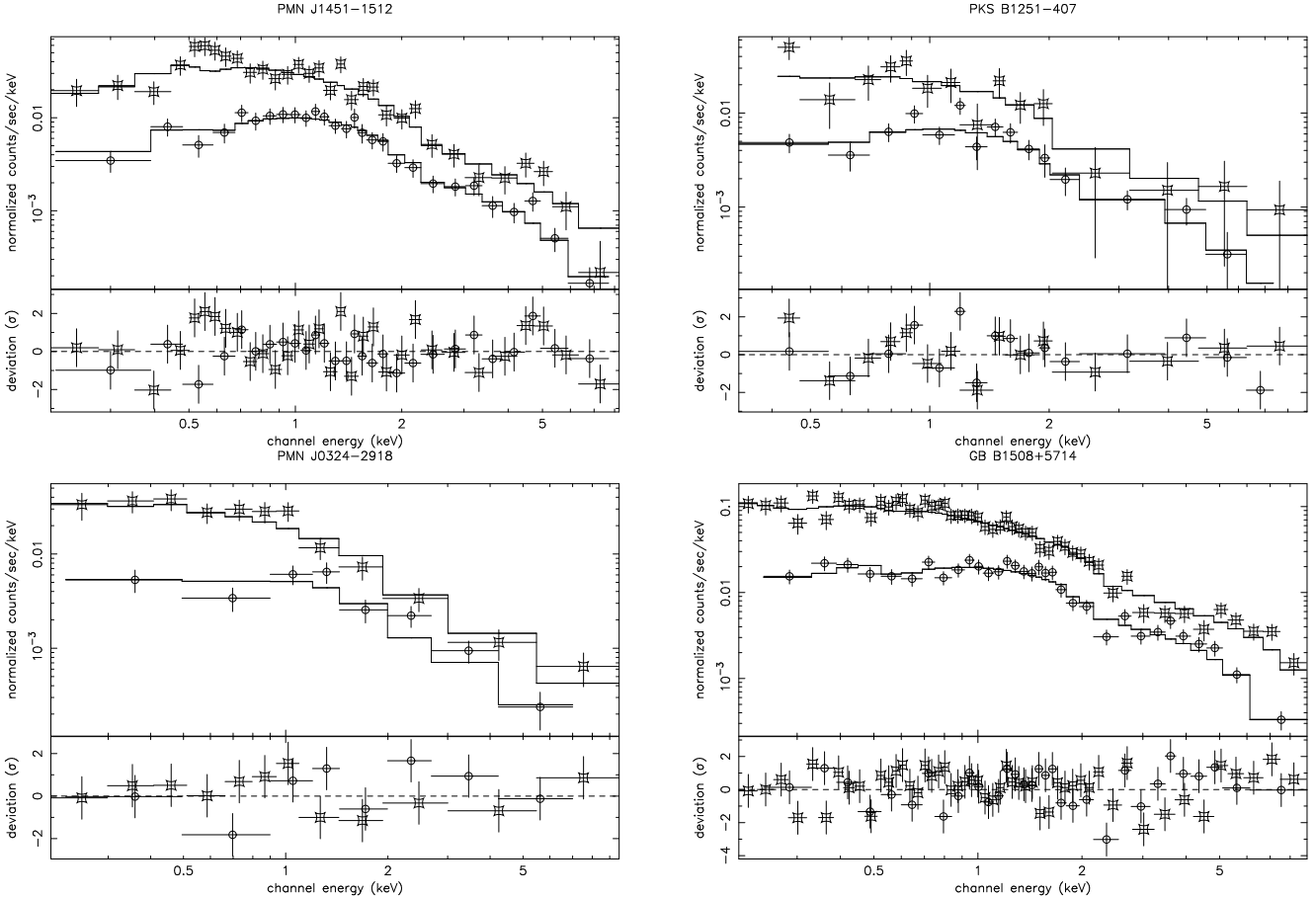


Figure 1. The spectra of the four objects measured with the PN (squares) and the combined MOS1 and MOS2 (circles) detectors. The model is the best-fit power-law with Galactic absorption to the joint PN and MOS spectra, and the residuals are the deviations in units of σ .

2.3 X-ray variability

The X-ray light curves of the sources were extracted within the observational intervals which were free from background flares. None of the objects show significant variability on such timescales as short as about 10 ksec, i.e. ~ 2 ksec in the quasar rest frames. For PMN J1451-1512 and GB B1508+5714, opportunities for exploring long-term variability are provided by multi-epoch observations and/or

by previous missions. The two observations of PMN J1451-1512, separated by 5 months, show no variability in either flux density or spectral index over the intrinsic time span of about one month in the quasar rest frame. Using the results from the literature and this work, the long-term light curve for GB B1508+5714 was constructed and is shown in Fig. 4 as the flux normalisation at 1 keV. The quasar was not detected in the ROSAT All-sky Survey (RASS), and an

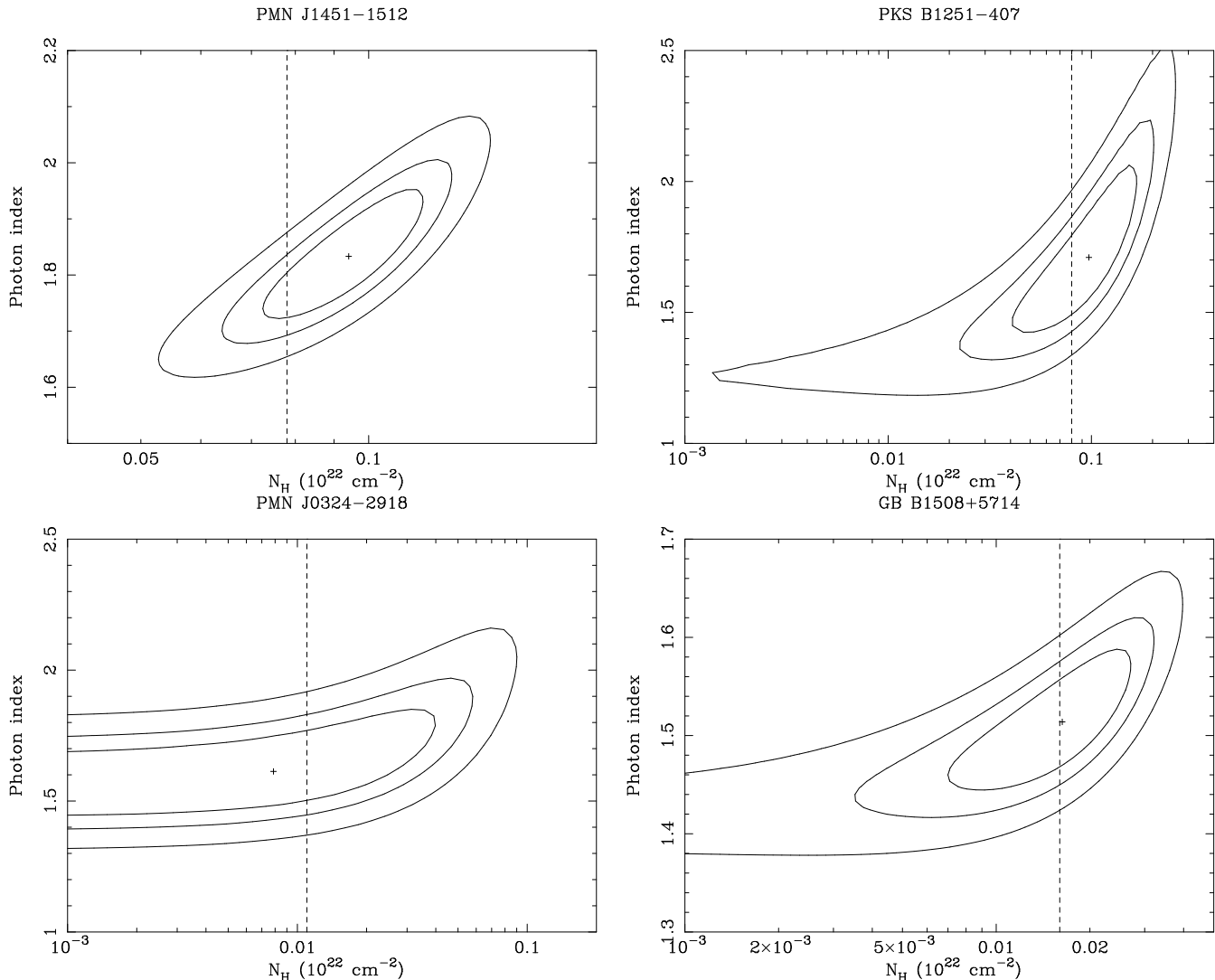


Figure 2. Confidence contours for the fitted spectral photon index and the equivalent column density of neutral Hydrogen as two interesting parameters. The contours correspond to the confidence levels of 68, 90, and 99 per cent, respectively. The cross represents the best-fit values. The vertical lines indicate the Galactic column densities.

X-ray flux limit was calculated using the X-ray background image and the exposure map at the quasar position. A photon index Γ 1.5 is assumed when converting the count rates into fluxes for both the *RASS* and *Einstein* observations. Long-term X-ray variability is evident on time scales of a few years (quasar rest frame). The large decrease of the X-ray flux observed with *ASCA* at 9 months (1.7 month in the quasar rest frame) apart was already reported by Moran & Helfand (1997) previously, which was accompanied by spectral flattening (Γ from 1.55 to 1.25). This decrease is confirmed by the later *Chandra* and *XMM-Newton* observations as reported here. Compared to the first *ASCA* observation, the photon indices found in the *XMM-Newton* and *Chandra* observations are similar to the *ASCA* value, but the flux density dropped by about 50 per cent.

3 DISCUSSION: X-RAY PROPERTIES OF $Z > 4$ RADIO-LOUD SAMPLE

We discuss in below the X-ray properties of the objects listed in Table 1 as a class. They form a significant subset with good X-ray spectroscopic data of the flux-limited sample of radio-loud quasars at $z > 4$.

3.1 Intrinsic X-ray absorption

In contrast to the previously detected excess X-ray absorption in GBB1428+4217 (Boller et al. 2000, Fabian et al. 2001b, Worsely et al. 2004b), PMN J0525-3343 (Fabian et al. 2001a, Worsely et al. 2004a), and RX J1028.6-0844 (Yuan et al. 2000, 2005), three out of the four quasars reported in this paper do not show X-ray absorption down to sensitivity limits comparable to, or even lower than, the N_H values found in the three ‘absorbed objects’ above (a few times 10^{22} cm^{-2} for ‘cold’ absorber). Tentative evidence for X-ray absorption is suggested in the remaining object PMN J1451-

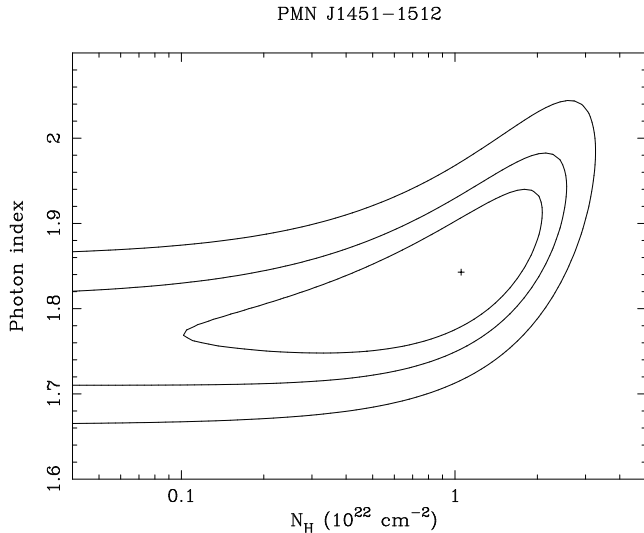


Figure 3. Confidence contours for the column density of intrinsic absorber versus photon index for PMN J1451-1512. The fit was performed jointly to the data from all the detectors from two observations. The abundances are assumed to be solar. The contours correspond to the confidence levels of 68, 90, and 99 per cent, respectively. The cross represents the best-fit values.

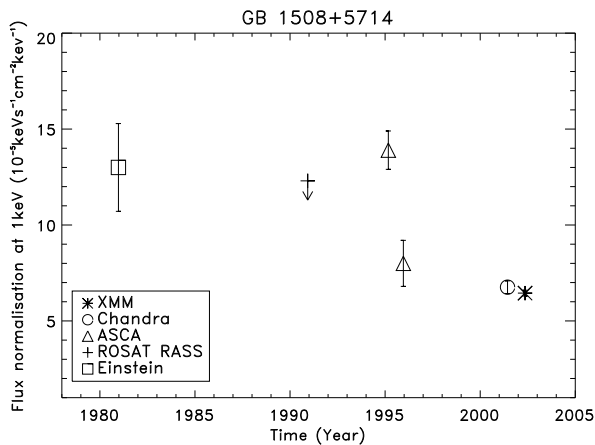


Figure 4. Long-term light curve for GB B1508+5714 (as the flux normalisation at 1 keV) shows strong variability. The arrow denotes an upper limit placed by the RASS. The previous data were taken from observations with *Einstein* (Mathur & Elvis 1995), *ASCA* (Moran & Helfand 1997), and *Chandra* (Yuan et al. 2003, Siemiginowska et al. 2003).

1512 with a N_{H} value of $1.0(\pm 0.6) \times 10^{22} \text{ cm}^{-2}$, though the significance is not high. We show in Fig. 5 (upper panel) the histogram of the N_{H} and upper limits of intrinsic X-ray absorption derived by assuming neutral absorber. A few implications can be inferred directly from Fig. 5, though the statistics may be affected by the small number of objects to some extent.

Firstly, X-ray absorption is detected in about half of the sample (3/7 or 4/7). Secondly, though with sparse data points, the small dispersion of the derived N_{H} values for the detected absorption is remarkable; for ‘cold’ absorber, they are around a few times 10^{22} cm^{-2} . The upper-limit for GB B1508+5714 as $3.3 \times 10^{21} \text{ cm}^{-2}$ is among the most

stringent constraints on excess N_{H} obtained so far in high- z quasars which do not show excess absorption. Yet it is not clear whether there exists a distinct sub-class which shows little or no X-ray absorption ($N_{\text{H}} \ll 10^{22} \text{ cm}^{-2}$), or there is a continuous N_{H} distribution with the non-detections falling into the lower N_{H} end (see Fig. 5). The observational difficulty lies in that at such high redshifts part of the absorption features, which are strong at low energy bands, is likely to be shifted out of the bandpass of the detectors and renders absorption with small N_{H} difficult to detect; this detection bias cannot be ruled out from the current X-ray data. Further X-ray observations for more objects and with better spectral quality are needed to test these possibilities, as well as to examine the ionisation parameter of the absorber, which is poorly constrained in current studies. If proves to be true, the narrow distribution of the absorption N_{H} in strong radio-loud quasars at $z > 4$ may suggest a common origin of the absorbers, which may also share similarities in some other physical properties, such as metallicity and ionisation parameter.

A comparison of the N_{H} distribution in our $z > 4$ sample with those observed at lower redshifts could reveal whether and how the intrinsic X-ray absorption property evolves with cosmic time. To make sure that the comparison is free from possible cross-calibration problems among different missions (see e.g. Yuan et al. 2005), we restrict ourselves to results obtained from *XMM-Newton* EPIC observations only. The lower panel in Fig. 5 shows the N_{H} distribution for a sample of $2 < z < 4$ highly radio-loud quasars observed with *XMM-Newton* collected from the literature (Page et al. 2005, Ferrero & Brinkmann 2003, Piconcelli & Guainazzi 2005). The results show that, at least for those with detected absorption, the N_{H} distribution in the redshift range 4–5 is largely consistent with that in $z=2$ –4, though the latter might be somewhat broader than the former. The fraction of objects in which X-ray absorption is detected is 50 per cent, similar to that in the $z=4$ –5 range obtained above in this work. These two pieces of evidence imply that the absorber probably underwent little or no cosmic evolution in the redshift range from $z=5$ to ~ 2 .

At even lower redshifts (below $z \sim 2$), we consider the N_{H} distribution for a sample of radio-loud AGN with *XMM-Newton* data given in Galbiati et al. (2005), the majority of which have $z < 2$. The N_{H} values given in the Galbiati et al. (refer to their Fig. 5) sample are well below⁵ 10^{22} cm^{-2} and are distributed widely in the $10^{19.5-22} \text{ cm}^{-2}$ range. Therefore, compared to low redshifts $z < 2$, an extension or even a systematic shift toward higher values is indicated in the N_{H} distribution at redshifts above $z \sim 2$. This trend can be seen clearly in Fig. 6, in which the absorption column densities are plotted versus redshifts for the objects concerned here. Exercising a non-parametric correlation test which takes into account the upper limits yielded the probability level of 0.005 (Kendall’s tau, using the ‘Astronomy Survival Analysis’ (Isobe, Feigelson & Nelson 1986)). A significant $N_{\text{H}} - z$ correlation is thus confirmed over the whole

⁵ One object with N_{H} above 10^{22} cm^{-2} in their figure is a type II radio-quiet one and is thus ignored. It should be noted that this sample is X-ray selected and is heterogeneous in terms of the radio power.

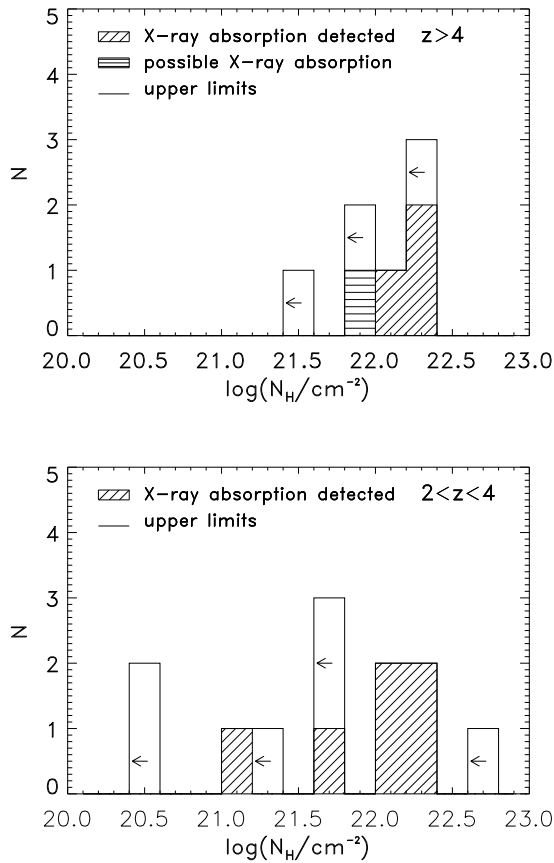


Figure 5. Histogram of the equivalent Hydrogen column densities for absorber associated with the quasars (at the quasar redshifts) for the samples of radio-loud quasars with good X-ray spectroscopic data in the redshift range of $z > 4$ (upper panel; from this work) and of objects in $2 < z < 4$ (lower panel; from Page et al. 2005). The detected column densities are represented by hatched regions while the upper limits (non-detections) by open lines. Neutral absorption is assumed with the solar metallicity; the actual column densities are higher if the absorbers are ionised.

$z = 0-5$ range. This is in line with the results claimed previously in the redshift range of $z < 4$ (Introduction; see also e.g. Page et al. 2005). The increase in N_H with redshift seems to happen at redshifts around 2, below and above which no correlation is found from the data, respectively. Furthermore, the fraction of radio-loud quasars showing X-ray absorption is much lower at redshifts $z < 2$ (< 10 per cent, see e.g. Fig. 2 in Yuan & Brinkmann 1999, see also Brinkmann et al. 1997) than the high percentage (~ 50 per cent) as found at redshifts above 4 in this work. These results, on both the fraction of objects with X-ray absorption and the N_H distribution, indicate a strong cosmic evolution effect in the X-ray absorption property of radio-loud quasars, which seems to occur at redshifts somewhere around 2.

Fig. 7 shows the distribution of the apparent luminosities (under the assumption of isotropic radiation) in the 1–50 keV band for the sample objects, with the different X-ray absorption properties marked respectively. Interestingly, there seems to be a systematic difference in X-ray luminosities spanning more than one order of magnitude;

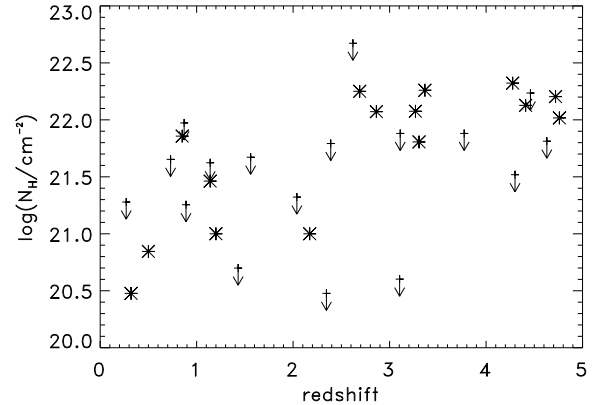


Figure 6. X-ray absorption column density N_H (assuming neutral gas) as a function of redshift. The data points for $z > 4$ objects are taken from this work, Yuan et al. (2005), and Worsley et al. (2004ab); those in $2 < z < 4$ are from Page et al. (2005) and those in $z < 2$ from Galbiati et al. (2005). For objects without detected X-ray absorption, the upper limits on N_H are indicated as arrows. The $N_H - z$ dependence is significant.

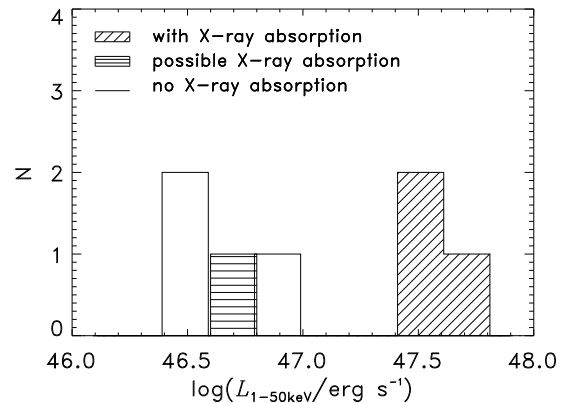


Figure 7. Distributions of the 1–50 keV X-ray luminosities (quasar rest frame, assuming isotropic radiation) for the sample objects, with their X-ray absorption status indicated.

X-ray absorption tends to be associated with objects with relatively high luminosities. It should be noted that this tendency should not be largely affected by flux variability, since the variability amplitudes are typically less than a factor of a few. This could be due, at least partly, to the small number of objects used and/or selection effects. The latter comes into play since, in general, lower source fluxes result in poorer X-ray spectra, from which X-ray absorption becomes more difficult to detect. More observational data are needed to improve the statistics and to eliminate the possible detection biases. If this trend is true, it may give some insight into the nature of the X-ray absorbers.

3.2 Broad band X-ray continuum emission

The distribution of the power-law photon indices Γ (obtained by taking into account excess X-ray absorption, if

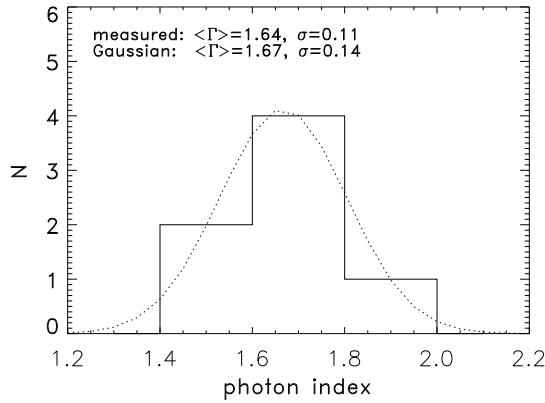


Figure 8. Histogram of the power-law photon indices for the sample. In the cases where soft X-ray spectral flattening is present, it is accounted for by intrinsic absorption. The dotted curve is a fitted Gaussian distribution.

present, see Table 3) for the sample is shown in Fig. 8. The measurement uncertainties are mostly $\lesssim 0.1$, smaller than the typical amplitudes of long-term variability in spectral slope ($\Delta\Gamma \sim 0.2$ – 0.3 ; see e.g. Moran & Helfand 1997, Yuan et al. 2005). We find a mean value of $\langle \Gamma \rangle = 1.64$ with a standard deviation $\sigma = 0.11$. A fit with a Gaussian distribution (dotted curve) gives $\langle \Gamma \rangle = 1.67$ and $\sigma = 0.14$. A comparison with low- z objects (e.g. Reeves & Turner 2000) indicates little or no evolution in the continuum spectral slope for radio-loud quasars from epochs of $z > 4$ to the present time. A tentative excess emission feature in the rest-frame 5–10 keV band was suggested to be similarly present in GB B1428+4217, PMN J0525-3343, and RX J1028.6-0844 (Worsley et al. 2004b, Yuan et al. 2005); however, its presence in the four newly observed objects reported here could not be tested due to the relatively low quality of their spectra.

Time variability is found to be common. In most objects with more than one observation by either *XMM-Newton* or other instruments, the broad band X-ray fluxes (1–50 keV in the quasar rest frame) appear to vary on timescales of a few months to years in the quasar rest frame, with amplitudes ranging from 10 percent (e.g. PMN J0525-3343) to a factor of 2 (GB B1508+5714). Such variations were often accompanied by changes in the spectral slopes with amplitudes of 0.2–0.3 (in RX J1028.6-0844 and GB B1508+5714), or even higher (in GB B1428+4217). No variations on timescales shorter than observation intervals, typically ~ 10 hours, were observed. The shortest timescale of variability found was about 7 days in GB B1428+4217, with an amplitude of ~ 10 per cent (Worsley et al. 2004b). The apparently extremely high X-ray luminosities and their short timescale variability suggest a blazar-like nature of these objects, as discussed in details elsewhere (e.g. Fabian et al. 1997, 1998; Moran & Helfand 1997).

ACKNOWLEDGEMENTS

WY acknowledges the support by the National Natural Science Foundation of China (NSF-10533050) and the BaiRen-

JiHua programme of the Chinese Academy of Sciences. ACF thanks the Royal Society for their support. This research has made use of the NASA/IPAC Extragalactic Database (NED) which is operated by the Jet Propulsion Laboratory, California Institute of Technology, under contract with the National Aeronautics and Space Administration.

REFERENCES

- Bassett L.C., Brandt W.N., Schneider D.P., Vignali C., Chartas G., Garmire G.P., 2004, *AJ*, 128, 523
 Boller Th., Fabian A.C., Brandt W.N., & Freyberg M.J., 2000, *MNRAS*, 315, L23
 Brinkmann W., Yuan W., Siebert J., 1997, *A&A*, 319, 413
 Cappi M., Matsuoka M., Comastri A., et al., 1997, *ApJ*, 478, 492
 Elvis M., Fiore F., Wilkes B., McDowell J., Bechtold J., 1994, *ApJ*, 422, 60
 Elvis M., Fiore F., Giommi P., Padovani P., 1998, *ApJ*, 492, 91
 Fabian A.C., Brandt W.N., McMahon R.G., Hook I.M., 1997, *MNRAS*, 291, L5
 Fabian A.C., Iwasawa K., Celotti A., et al., 1998, *MNRAS*, 295, L25
 Fabian A.C., Celotti A., Iwasawa K., McMahon R.G., Carilli C.L., Brandt W.N., Ghisellini G., Hook I.M., 2001a, *MNRAS*, 323, 373
 Fabian, A.C., Celotti, A., Iwasawa K., Ghisellini G., 2001b, *MNRAS*, 324, 628
 Ferrero E. & Brinkmann W., 2003, *A&A*, 402, 465
 Fiore F., Elvis M., Giommi P., Padovani P., 1998, *ApJ*, 492, 79
 Fiore F., Elvis M., Maiolino R., Nicastro F., Siemiginowska A., Stratta G., D’Elia V., 2003, *A&A*, 409, 57
 Galbiati E., Caccianiga A., Maccacaro T., Braitto V., Della Ceca R., et al. 2005, *A&A*, 430, 927
 Grupe D., Mathur S., Wilkes B., Osmer P., 2006, *AJ*, 131, 55
 Hook I.M., McMahon R.G., Patnaik A.R., Browne I.W.A., Wilkinson P.N., Iwrin M.J. and Hazard C., 1995, *MNRAS*, 273, L63
 Hook I.M. & McMahon R.G., 1998, *MNRAS*, 294, L7
 Hook I.M., McMahon R.G., Shaver P.A., Snellen I.A.G., 2002, *A&A*, 391, 509
 Isobe T., Feigelson E.D., Nelson P.I., 1986, *ApJ*, 306, 490
 Loiseau N., 2004, ‘User’s guide to the XMM-Newton Science Analysis System’, (issue 3.1), XMM-Newton Science Operation Center (<http://xmm.vilspa.esa.es/sas/>)
 Ma C., Arias E.F., Eubanks T.M., Fey A.L., Contier A.-M., et al. 1998, *AJ*, 116, 516
 Mathur S. & Elvis M., 1995, *AJ*, 110, 1551
 Moran E.C. & Helfand D.J., 1997, *ApJL*, 484, 95
 Page K.L., Reeves, J.N., O’Brien P.T., Turner M.J.L., 2005, *MNRAS*, 364, 195
 Piconcelli E. & Guainazzi M., 2005, *A&A*, 442, L53
 Reeves J.N. & Turner M.J.L., 2000, *MNRAS*, 316, 234
 Schwartz D.A., 2002, *ApJL*, 569, 23
 Shaver P.A., Wall J.V., Kellermann K.I., 1996, *MNRAS*, 278, L11
 Siemiginowska A., Smith R.K., Aldcroft T.L., Schwartz D.A., Paerels F., Petric, A.O., 2003, *ApJL*, 598, 15

- Snellen, I. A. G., McMahon, R. G., Dennett-Thorpe, J.
2001, MNRAS, 325, 1167
- Vignali C., Brandt W.N., Schneider D.P., Anderson S.F.,
Fan X., et al., 2003, AJ, 125, 2876
- Vignali C., Brandt W.N., Schneider D.P., Kaspi S., 2005,
AJ, 129, 2519
- Wilkes, B.J., Elvis, M., Fiore, F., McDowell J., Tananbaum
H., Lawrence A., 1992, ApJL, 393, L1
- Worsley M.A., Fabian, A.C., Turner A.K., Celotti A., Iwa-
sawa K., 2004a, MNRAS, 350, 207
- Worsley M.A., Fabian, A.C., Celotti A., Iwasawa K., 2004b,
MNRAS, 350, L67
- Yuan, W. and Brinkmann, W., 1999, in Highlights in X-ray
Astronomy, ed., Aschenbach, B., and Freyberg, M., (MPE
Report 272), 240
- Yuan W., Matsuoka M., Wang T., Ueno S., Kubo H., Mi-
hara T., 2000, ApJ, 545, 625
- Yuan W., Fabian A.C., Celotti A., Jonker P.G., 2003, MN-
RAS, 346, L7
- Yuan W., Fabian A.C., Celotti A., McMahon R.G., Mat-
suoka M., 2005, MNRAS, 358, 432